Bone 43 (2008) 249–263

Contents lists available at ScienceDirect

Bone

journal homepage: www.elsevier.com/locate/bone

Model structure and control of bone remodeling: A theoretical study

Peter Pivonka [a], Jan Zimak [a], David W. Smith [a,*], Bruce S. Gardiner [a], Colin R. Dunstan [b], Natalie A. Sims [c], T. John Martin [c], Gregory R. Mundy [d]

[a] Department of Civil and Environmental Engineering, University of Melbourne, VIC 3010, Australia
[b] Bone Biology Unit, ANZAC Research Institute, Concord, NSW 2139, Australia
[c] Department of Medicine at St. Vincent's Hospital, University of Melbourne, VIC, 3065, Australia
[d] Center for Bone Biology, Vanderbilt University, Nashville, 37232-0575, USA

ARTICLE INFO

Article history:
Received 12 October 2007
Revised 31 January 2008
Accepted 17 March 2008
Available online 15 April 2008

Edited by: Dr. R. Baron

Keywords:
Bone remodeling
Osteoblast–osteoclast interactions
TGF-β
Cell population dynamics
Model structure and control of bone remodeling

ABSTRACT

It is generally accepted that RANKL is highly expressed in osteoblast precursor cells while OPG is highly expressed in mature osteoblasts, but to date no functional utility to the BMU has been proposed for this particular ligand–decoy–receptor expression profile. As discovered in the mid 90s, the RANK–RANKL–OPG signaling cascade is a major signaling pathway regulating bone remodeling. In this paper we study theoretically the functional implications of particular RANKL/OPG expression profiles on bone volume. For this purpose we formulate an extended bone–cell dynamics model describing functional behaviour of basic multicellular units (BMUs) responsible for bone resorption and formation. This model incorporates the RANK–RANKL–OPG signaling together with the regulating action of TGF-β on bone cells. The bone–cell population model employed here builds on the work of Lemaire et al. (2004) [1], but incorporates the following significant modifications: (i) addition of a rate equation describing changes in bone volume with time as the key 'output function' tracking functional behaviour of BMUs, (ii) a rate equation describing release of TGF-β from the bone matrix, (iii) expression of OPG and RANKL on both osteoblastic cell lines, and (iv) modified activator/repressor functions. Using bone volume as a functional selection criterion, we find that there is a preferred arrangement for ligand expression on particular cell types, and further, that this arrangement coincides with biological observations. We then investigate the model parameter space combinatorially, searching for preferred 'groupings' of changes in differentiation rates of various cell types. Again, a criterion of bone volume change is employed to identify possible ways of optimally controlling BMU responses. While some combinations of changes in differentiation rates are clearly unrealistic, other combinations of changes in differentiation rates are potentially functionally significant. Most importantly, the combination of parameter changes representing the signaling pathway for TGF-β gives a unique result that appears to have a clear biological rationale. The methodological approach for the investigation of model structure described here offers a theoretical explanation as to why TGF-β has its particular suite of biological effects on bone–cell differentiation rates.

Introduction

Bone remodeling is the continuous process of bone resorption and bone formation occurring in the skeleton of vertebrates throughout their lifetime [2]. Remodeling occurs asynchronously at multiple spatially and temporally discrete sites of the skeleton in order to remove portions of damaged or older bone, replacing this with newly formed bone. The purpose of bone remodeling is to [3]: (i) repair of micro-factures that may lead to macroscale fatigue fractures under repeated cyclic loading (i.e. sometimes referred to as 'targeted remodeling' [4]) and (ii) mineral homeostasis, by providing access to stores of calcium and phosphate (i.e. sometimes referred to as 'random remodeling' [5]). Remodeling is accomplished by groups of bone forming cells (osteoblasts) and bone resorbing cells (osteoclasts), which work together in so-called 'basic multicellular units' (BMUs) [3,6]. The three stages in a BMU's lifetime are activation (A), resorption (R), and formation (F) (followed by a quiescent stage). The resorption process is followed by a reversal phase before osteoblasts enter the remodeling site. Many bone disorders such as osteoporosis, Paget's disease and bone diseases of cancer can be ascribed to imbalances in the ARF cycle of bone remodeling [7]. A BMU consists of cells of the osteoblastic and osteoclastic lineage at various stages of maturation. Whereas osteoblasts are derived from mesenchymal stem cells located in the bone marrow, spleen or liver, osteoclasts are derived from hematopoietic stem cells. Depending on the gene expression profiles and/or cell markers, various stages of maturation of these cell lines can be distinguished [8–10].

Current knowledge of bone remodeling is primarily based on experimental observations. A thorough search of the literature reveals

* Corresponding author.
E-mail address: david.smith@unimelb.edu.au (D.W. Smith).

8756-3282/$ – see front matter © 2008 Elsevier Inc. All rights reserved.
doi:10.1016/j.bone.2008.03.025

a vast amount of research on various endocrine, paracrine, and autocrine interactions involving receptors and ligands. Based on these observations, a large number of hypotheses have been postulated regarding bone–cell communication and the role played by various receptor–ligand pathways. However, due to the complexity of the bone regulatory system and the numerous factors and interactions involved, understanding 'system behaviour' is still fragmentary. Discovery of a major signaling pathway (i.e., RANK–RANKL–OPG pathway) in the mid 90s has revealed that a large number of hormones and therapeutic drugs exert their physiological effect through this cell–cell interaction pathway [11–13]. Increasingly, experimental data on signaling mechanisms between bone cells indicates that interactions are complex, and drawing conclusions based on intuition alone may be very difficult, and quite possibly misleading.

Mathematical modeling provides a powerful tool to reduce ambiguity as to causes and effects in complex systems, and allows one to test various experimental and theoretical hypothesis 'in-silico' [14,15] — hypotheses that may be difficult or impossible to test in-vitro or in-vivo. Given this context, it is perhaps surprising that there have been relatively few mathematical models proposed that study the integrated effects of known bone–cell interactions. However, there have been some recent papers. For example the role of parathyroid hormone (PTH) on bone formation/resorption has been investigated by several researchers [16–18], while mathematical models of bone cell dynamics have been proposed by Komarova et al. [19] and Lemaire et al. [1]. In the model of Komarova et al. [19] biochemical signaling between active osteoclasts and osteoblasts has been taken into account in a rather abstract way originally proposed by Savageau [20]. In this approach, all factors leading to a cell response are lumped together in a single exponential parameter. In contrast, the model of Lemaire et al. [1] has incorporated known physiologic regulatory mechanisms like the RANK–RANKL–OPG pathway, together with other factors describing cell communication between osteoblastic and osteoclastic cell lines at various stages of maturation. Both of the above cited models allow quantitative investigation of various aspects on bone remodeling, including the effectiveness of current bone therapies and verification of hypotheses. However, as far as we are aware, no previous papers on bone biology have investigated the model structure of cell–cell interactions theoretically.

In this paper we develop an extended bone–cell population model based on the work of Lemaire et al. [1]. Motivated by the current bone biology literature, the following additional features have been incorporated into the new model: (i) a rate equation describing changes in bone volume,[1] (ii) a rate equation describing TGF-β concentration as function of resorbed bone volume, (iii) RANKL and OPG expression on osteoblastic cells at different stages of maturation, and (iv) new activator/repressor functions based on enzyme kinetics. This new model is then employed to investigate optimal model structures for RANKL and OPG expression on osteoblastic cells at different stages of maturation. Having found an optimum for the model structure, we then scan through combinations of parameters controlling differentiation of different cell types, searching for optimal changes in differentiation rates that may lead to effective functional control in an active BMU. This leads us to suggest a reason as to why TGF-β has its constellation of biological effects on cell lineages in a BMU, which has been discovered through the combined efforts of many experimental biologists [21].

The mathematical model describing bone regulation

The 'cell population model' considered in this paper describes the temporal changes of bone–cell populations during the remodeling process, averaged over a volume of bone of sufficient size such that averaging gives consistent results. This abstract model does not refer to a single BMU. As such the cell numbers in the model represent spatial averages over a finite volume of bone, where the volume of bone contains many BMUs. It is noted that this type of model contrasts with a model of a single BMU where both spatial and temporal sequences defines what type of bone cells are present (e.g., formation of osteoclasts always precedes osteoblast formation).

The cell population model is initially run to reach a steady state, and then the model is perturbed from this steady state, and the way the model responds to the perturbation is the primary source of interest in this paper. As stated in the previous paragraph, at a particular time instant, one observes active osteoclasts and osteoblasts in a volume of bone. These cells can be associated with a certain average amount of bone being resorbed and laid down. The difference between bone resorption and formation is referred to as the 'bone balance'. In our mathematical modeling approach we are interested in the ways the bone balance is influenced by the model structure. Applying perturbations to the system (such as changing differentiation and apoptosis rates) we are able to address this question. Based on the model results we can then estimate the sensitivity of the bone remodeling process (or BMUs) to changes in bone microenvironment associated with changes of cell characteristics. As this model starts from an initial steady state for bone remodeling (associated with zero bone balance) a perturbation leads to changes in bone balance. When the perturbing influence is removed a new steady state is reached. Hence, the temporal evolution of model variables does not represent an individual bone remodeling cycle. Questions related to activation (or origination) and termination of individual BMUs are beyond the scope of this paper.

Now it could be argued that the spatial arrangements of osteoclasts in a BMU do impact on the population-level model. For such cases additional information needs to be included in the model. Often complex processes cannot be described by a single model, and so an idea in computational analysis occupying researchers at the current time is to have a hierarchy of models, that is, have models nested one within one another. We have used this approach, by including a model of ligand–receptor interaction nested within a cell–cell interaction model. Generally, at the lower scales more information can be included, but as one moves up through the length and time scales, averaging needs to be used. While averaging always loses information, this is not necessarily a negative. Averaging simplifies the problem, and makes it computationally tractable (for example, it is simply not possible to model the entire skeleton and all the BMUs contained therein), while retaining the aspects of interest. The task of the modeler is to achieve the right balance between excessive model complexity (i.e. that does not provide any additional insight and often obscures the things of interest), and oversimplification, such that the model does not answer the questions of interest in a helpful way.

Biochemical mechanisms

The cell population dynamics model including biochemical mechanisms of receptor–ligand interactions is shown schematically in Fig. 1. Given the large number of different cell types involved in active bone–cell differentiation, only a representative subset of cell types are included in the model. As a minimalist realistic approximation, four cell types of the osteoblast lineage (with two being state variables) and three cell types of the osteoclast lineage (with one being a state variable) are considered here. This is clearly a simplification of the actual biological system, and relaxing these assumptions is one way in which a more realistic analysis will be achieved in the future.

The *osteoblastic lineage* derives from a large pool of mesenchymal stem cells capable of differentiating into various cells such as osteoblastic cells, chondrocytes, adipocytes, etc [8]. Here we denote this pool of cells as uncommitted osteoblast progenitors (OB_u). Once,

[1] The term rate equation refers to an equation which describes changes of a variable with time.

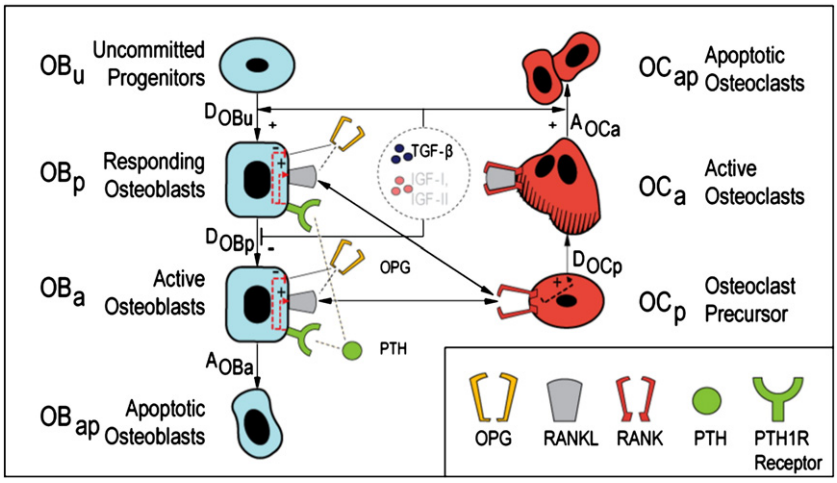

Fig. 1. Schematic illustration of bone–cell population model: (a) osteoblastic cell line and (b) osteoclastic cell lines taken into account together with RANK–RANKL–OPG pathway (D_{OB}, D_{OC}…differentiation rates of osteoblasts and osteoclasts; E_{OB}, E_{OC}…elimination/apoptosis rates of osteoblasts and osteoclasts; RANKL binds to RANK and promotes differentiation of OC_p; OPG binds to RANKL and so inhibits OC_p differentiation).

these cells commit to the osteoblast lineage they are generally denoted as 'responding' or 'preosteoblasts' (OB_p). This cell type is not a single cell type but rather a composite of various phenotypes that share similar characteristics. Both OB_u and OB_p are early osteoblasts and highly responsive to differentiation either directly through growth factors (e.g. TGF-β) or indirectly through other regulatory factors (e.g. PTH) [9]. After creation of a 'pool' of active osteoblasts (OB_a) bone formation can proceed in the remodeling cycle [3]. The rate of bone formation is assumed to be proportional to the number of active osteoblasts. Experimental data suggests that this pool of active osteoblasts is under close control of the osteoclasts [2]. At the end of the osteoblast cell cycle osteoblasts either undergo apoptosis (i.e., cell death) or form osteocytes or lining cells at bone surfaces. In the current model only the apoptotic state is considered.

The second cell line considered in the model are osteoclasts, the only cell type in the body capable of resorbing bone [22]. Osteoclasts derive from hematopoietic progenitor cells, here denoted as uncommitted osteoclast progenitors (OC_u), to become osteoclast precursors cells (OC_p) [10,23]. Macrophage colony stimulating factor (M-CSF, also called CSF-1) has been shown to be absolutely essential for early commitment of hematopoietic progenitors to the osteoclast lineage [24]. Once committed, M-CSF together with the receptor activator of nuclear factor kappa beta (NF-κβ) ligand (known as RANKL) are required for differentiation of osteoclast precursor cells into more mature osteoclastic cells. Final differentiation of osteoclast precursors into active osteoclasts (OC_a's) is promoted by RANKL [10]. RANKL binds to the receptor activator of NF-κβ (known as RANK) expressed on osteoclast precursor cells (OC_p). In the model, bone resorption is assumed to be proportional to the number of active osteoclasts (OC_a). After the resorption process is complete active osteoclasts undergo apoptosis.

RANK–RANKL–OPG signaling

It had been hypothesized for many years that osteoclast development and activity were under the control of osteoblasts/stromal cells [7]. However, details of the molecular and physiological control mechanisms had not been identified until the end 90s. Discovery of three members of the Tumor Necrosis Factor (TNF) superfamily finally resolved this problem [25]. Receptor activator of nuclear factor kappa beta (NF-κβ) ligand (RANKL) is a protein found on the surface of cells of the osteoblastic cell lineage, which may also be cleaved into a soluble form by metalloprotease. RANKL interacts with its receptor, RANK, expressed on the surface of hematopoietic precursor cells, thereby promoting osteoclast formation (as well as maintaining their viability and activity) [11]. The interaction of RANKL/RANK is regulated by the soluble decoy ligand, osteoprotegrin (OPG), also produced by stromal/osteoblastic cells. OPG binds to RANKL to prevent RANKL stimulation of RANK expressed by osteoclasts. This signaling pathway is now known as the RANK–RANKL–OPG pathway.

It has been found that many factors regulating resorption such as parathyroid hormone (PTH), prostaglandins, interleukins, vitamin D_3, and corticosteroids all signal to the osteoblast/stromal cells, which then translate these signals into different levels of RANKL and OPG expression, which in turn control osteoclast formation [11,26]. So important is the control mechanism of RANKL/OPG levels by cytokines and hormones, that it has been described as the '*convergence hypothesis*' [27]. Important physiological effects for many bone diseases including osteoporosis, Paget's disease, tumor metastasis, humoral hypercalcemia of malignancy, and multiple myeloma, can be explained through imbalances in RANKL/OPG ratio [7,12,24,28,29].

Two principal *systemic hormones* regulating osteoclast formation are parathyroid hormone (PTH) and vitamin D_3 ($1,25(OH)_2D_3$). Receptors for these hormones are only expressed on osteoblasts. In other words, these hormones indirectly stimulate osteoclast formation via osteoblasts, which in turn regulates mineral homeostasis. The third hormone involved in mineral regulation is calcitonin (CT), which acts directly on osteoclasts as an antagonist to the action of PTH and vitamin D_3, inhibiting bone resorption.

It is well known that the bone matrix serves as a large reservoir for storage of *growth factors* such as TGF-β and IGFs [23,30]. During resorption of bone matrix by active osteoclasts these factors are released into the microenvironment of BMUs and act as 'self-regulating' agents on bone cells [31]. In a recent review, the action of TGF-β on bone cells has been analyzed with special emphasis on the bone–cell microenvironments [21].

Note that in the current version of the model we only consider the action of TGF-β on bone cells (i.e., binding of TGF-β to its receptors on osteoblasts and osteoclasts). This can be taken into account by means of activator and/or repressor functions depending on the action of TGF-β. Measurement of TGF-β in dried bone powder has revealed rather high concentrations, approximately 1000-fold higher than the levels required for cell responses of osteoblasts [32,33]. The action of TGF-β on osteoblasts depends on the state of cell maturation [34]. TGF-β stimulates differentiation of uncommitted osteoblast progenitors (OB_u), but it inhibits differentiation of osteoblast precursor cells (OB_p) [21]. Thus the action of TGF-β on osteoblastic cells leads to an increase of the pool of osteoblast precursor cells (OB_p), as shown in

Fig. 1. If, TGF-β is then removed from the system, or becomes inactivated, osteoblast precursor cells can differentiate to become active osteoblastic cells (OB_a). On the other hand, TGF-β has been found to promote osteoclast apoptosis [35]. We include the above described actions of TGF-β on bone cells. Exactly why TGF-β exhibits this constellation of actions on differentiation of various cell types is not functionally clear. In this paper we attempt to offer an explanation for the particular combination of biological actions of TGF-β on bone cells.

Bone–cell population dynamics model

As outlined above the cell population dynamics model considers the following three state variables[2]: osteoblast precursors (OB_p), active osteoblasts (OB_a), and active osteoclasts (OC_a). Numbers of uncommitted osteoblast progenitors (OB_u) and osteoclast precursor cells (OC_p) are assumed to be very large and constant and so are not modeled explicitly. A major difference of the model proposed here and the one presented by Lemaire et al. [1] is the consideration of the location of RANKL and OPG expression on osteoblastic cells. Lemaire et al. [1] assumes that RANKL is expressed only on active osteoblasts (OB_a) and OPG is only expressed on osteoblast precursor cells (OB_p). However experimental evidence suggests that the reverse may be the case [36–38]. In our model, we allow RANKL and OPG to be expressed on both active osteoblasts and osteoblast precursors at different expression levels, and seek to understand the functional effect of RANKL and OPG expression on different cell types (see Fig. 2). Furthermore, many of the mathematical functions describing biochemical regulation of bone–cell communication proposed in the original Lemaire et al. [1] model have been changed here, inspired by enzyme kinetics theory, which provides an appropriate framework for modeling [39,40], and a desire to have all reactions treated in a consistent way.

Modeling of activation and repression

Cell responses such as differentiation, proliferation, and apoptosis are all related to various receptor–ligand interactions. Some of these interactions are stimulating, while others are inhibiting. The same observations are true for production of molecules due to receptor–ligand interactions. Assuming that a cellular process is governed by a single factor X, we can express the rate of production Y per unit time as a function of the concentration X in it's active form, X^*:

$$Y = f(X^*) \tag{1}$$

Typically the (input) function $f(X^*)$ is a monotonic, S-shaped function, that is increasing when X is an activator and decreasing when X is a repressor. A commonly employed function describing many real gene and molecular input functions is the so-called 'Hill function'. Hill functions for activation and repression processes are given as [40]:

$$f(X^*) = \beta\pi_{act} = \frac{\beta(X^*)^n}{K_1 + (X^*)^n} \quad \text{Hill function for activator} \tag{2}$$

$$f(X^*) = \beta\pi_{rep} = \frac{\beta}{1 + \left(\frac{X^*}{K_2}\right)^n} \quad \text{Hill function for repressor} \tag{3}$$

where K_1 and K_2 (in mol/l) are activation/repression coefficients, β is the maximal expression level of the promoter, and n is the Hill coefficient governing the steepness of the input function π from monotonic S-shaped (for small n) to monotonic sigmoidal shaped (for large n). For enzyme kinetic studies K_1 and K_2 are assumed to be equal to the dissociation constant. However, for modeling of cell responses this is generally not the case. Here, we assume $n = 1$ if not otherwise specified.

[2] State variable expresses the fact that a particular state of a system (in this context the bone remodeling process) can be uniquely described by knowing the values of a set of key variables.

We will use the following indices for the input functions π: $\pi^{molecule}_{act/rep,cell}$ where "rep/act" identifies activator or repressor function, "cell" denotes the cell type a specific molecule binds to, and "molecule" denotes the ligand involved in a particular cell response.

Cell population dynamics model

Utilizing Fig. 1 we can formulate changes in cell populations over time as follows:

$$\frac{dOB_p}{dt} = D_{OB_u} \cdot \pi^{TGF-\beta}_{act,OB_u} - D_{OB_p} \cdot OB_p \cdot \pi^{TGF-\beta}_{rep,OB_p} \tag{4}$$

$$\frac{dOB_a}{dt} = D_{OB_p} \cdot OB_p \cdot \pi^{TGF-\beta}_{rep,OB_p} - A_{OB_a} \cdot OB_a \tag{5}$$

$$\frac{dOC_a}{dt} = D_{OC_p} \cdot OC_p \cdot \pi^{RANKL}_{act,OC_p} - A_{OC_a} \cdot OC_a \cdot \pi^{TGF-\beta}_{act,OC_p} \tag{6}$$

where D_{OB_u}, D_{OB_p} and D_{OC_p} are differentiation rates of uncommitted osteoblast progenitors, osteoblast precursor cells, and osteoclast precursor cells, respectively. $\pi^{TGF-\beta}_{act,OB_u}$, $\pi^{TGF-\beta}_{rep,OB_p}$ and $\pi^{TGF-\beta}_{act,OC_p}$ are the activator/repressor functions related to TGF-β binding to it's receptors on osteoblasts and osteoclasts. π^{RANKL}_{act,OC_p} is the activator function related to RANKL binding to it's receptor RANK expressed on osteoclast precursor cells (OC_p). A_{OB_a} and A_{OC_a} are the apoptosis rates of active osteoblasts and osteoclasts. Note that differentiation and apoptosis rates in this paper refer to absolute number of cells/unit time. The governing Eqs. (4)–(6) represent "cell balance" equations where changes of each cell population (i.e., OB_p, OB_a, and OC_a) are caused by addition and removal of cells of the respective lineage. Whereas addition of cells naturally occurs by proliferation and differentiation of precursor cells (or by external administration of cells), elimination of cells is caused by apoptosis (or by external extraction of cells). Differentiation and apoptosis are regulated by several activator and repressor functions, such as for example, TGF-β binding to its receptors on uncommitted osteoblast progenitors promoting their differentiation ($\pi^{TGF-\beta}_{act,OB_u}$), whereas TGF-β binding to its receptors on osteoblast precursor cells inhibiting their differentiation ($\pi^{TGF-\beta}_{rep,OB_p}$).

Apart from cell types and numbers of cells involved in the remodeling sequence, another essential parameter characterizing bone remodeling is the change of bone volume over time. This 'system output' can be estimated according to [41]:

$$\frac{dBV}{dt} = AF \cdot (-V_{res} + V_{form}) \tag{7}$$

where BV denotes the total bone volume and AF (in [1/t]) is the activation frequency of BMUs corresponding to the number of BMUs being formed in a unit volume per unit time, and V_{res} and V_{form} are the volume of resorption cavity and the deposited volume of completed osteon, respectively. It is well known that bone balance changes with age, i.e., whereas in young animals bone balance is positive leading to bone growth in aging animals bone balance is negative leading to bone loss and osteoporosis. In between these two cases there is supposedly a time span (or point) which may be viewed as "normal" were no bone is gained or lost. In this paper we start from the special case of zero bone (volume/mass) gain and loss (which corresponds to a horizontal tangent in the bone volume/mass vs. age curve). We have assumed that this would be the "steady state" for the young adult skeleton (i.e. constant bone volume independent of age).

Eq. (7) has two major components; activation frequency (i.e., the number of new BMUs being formed per unit time) and the bone remodeling balance. Riggs and Parfitt argue that AF is the probability that bone remodeling is initiated on any particular surface at any given time. It is the summation of several processes, most notably the recruitment and differentiation of osteoclasts from precursor cells.

Table 1
Biochemical binding reactions between ligands (A) and receptors (B) considered in the bone cell population model together with corresponding activator/repressor functions ([a]RANKL expressed on OB_p and OB_a, * on TGF-β receptors indicate different receptor properties)

Ligand A	Receptor B	B expressed on	Complex C	Activator/repressor functions
TGF-β	TGF-βR	OB_u	[TGF-β–TGF-βR]	$\pi^{TGF\text{-}\beta}_{act,OB_u}$
TGF-β	TGF-βR*	OB_p	[TGF-β–TGF-βR*]	$\pi^{TGF\text{-}\beta}_{rep,OB_p}$
TGF-β	TGF-βR**	OC_a	[TGF-β–TGF-βR**]	$\pi^{TGF\text{-}\beta}_{act,OC_a}$
PTH	PTH1R	OB_p and OB_a	[PTH–PTH1R]	π^{PTH}_{act,OB_p}, π^{PTH}_{act,OB_a}, π^{PTH}_{rep,OB_p}, π^{PTH}_{rep,OB_a}
RANKL	OPG	OB_p and OB_a	[RANKL–OPG]	–
RANKL	RANK	OB_p and OB_a	[RANKL–RANK]	π^{RANKL}_{act,OC_p}

Because AF varies among individuals and between disease states by up to 10-fold, activation frequency is a major drug target for bone remodeling. The other component of Eq. (7) is the remodeling balance, which is the algebraic difference between resorption and formation phase of bone turnover in a BMU. If the resorption cavity is on average underfilled by osteoblasts, the remodeling balance will be negative, whereas if it is on average overfilled it will be positive. Remodeling balance is estimated to vary among individuals and disease states by about ±10%, which is 1/100 of the variability of the activation frequency [41]. In the adult without bone mineral demands, normal bone physiology may then be defined as zero change in bone volume after a remodeling cycle.

In an alternative presentation, we may assume that bone deposition and bone resorption rate is proportional to the number of active bone cells, so we can reformulate Eq. (7) as:

$$\frac{d\mathrm{BV}}{dt} = -k_{\mathrm{res}}\,\widetilde{\mathrm{OC}}_{\mathrm{a}} + k_{\mathrm{form}}\,\widetilde{\mathrm{OB}}_{\mathrm{a}} \tag{8}$$

with

$$\widetilde{\mathrm{OC}}_{\mathrm{a}}(t) = \mathrm{OC}_{\mathrm{a}}(t) - \mathrm{OC}_{\mathrm{a}}(t_0) \quad \text{and} \quad \widetilde{\mathrm{OB}}_{\mathrm{a}} = \mathrm{OB}_{\mathrm{a}}(t) - \mathrm{OB}_{\mathrm{a}}(t_0) \tag{9}$$

Note that BV in Eq. (8) denotes normalized bone volume in [%] and k_{res} and k_{form} are the relative bone resorption and formation rates respectively. This representation allows us to link cell numbers (obtained from the cell population model Eqs. (4)–(6)) to changes in bone volume (Eq. (8)). Measurement of cell numbers in normal steady-state bone remodeling and measuring either k_{res} or k_{form} allows us to compute the remaining parameter from the requirement of zero changes of bone volume, i.e., $d\mathrm{BV}/dt = 0$ for bone not changing its total volume (see also comments to Eq. (7)). This state is referred here as the initial state t_0 (and has corresponding cell numbers $\mathrm{OC}_{\mathrm{a}}(t_0)$ and $\mathrm{OB}_{\mathrm{a}}(t_0)$). It is noted that k_{res} and k_{form} could be also obtained for cases of constant negative changes in bone volume. The numerical results using the latter assumption do not significantly differ from the zero changes in bone volume assumption and, hence, conclusions drawn from the case considered here are general.

Effects of TGF-β on bone cells

The osteoblast lineage originates from a large population of uncommitted progenitors (OB_u). These progenitors express a specific TGF-β receptor (TGF-βR in Table 1) which, once activated, leads to differentiation of these progenitors into preosteoblasts (OB_p). It is generally accepted that various types of growth factors such as TGF-β (IGF-I and IGF-II etc) are stored in the bone matrix and are released once bone is resorbed by active osteoclasts (OC_a). In our model we assume the release rate of TGF-β to be proportional to the rate of resorbed bone volume ($\dot{V}_{\mathrm{res}}$) and, hence, proportional to active osteoclasts:

$$\begin{aligned}\frac{d\mathrm{TGF}-\beta}{dt} &= \alpha\cdot\dot{V}_{\mathrm{res}} - \tilde{D}_{\mathrm{TGF}-\beta}\cdot\mathrm{TGF}-\beta + S_{\mathrm{TGF}-\beta}\\ &= \alpha\cdot k_{\mathrm{res}}\mathrm{OC}_{\mathrm{a}} - \tilde{D}_{\mathrm{TGF}-\beta}\cdot\mathrm{TGF}-\beta + S_{\mathrm{TGF}-\beta}\end{aligned} \tag{10}$$

where α is a proportionality constant expressing the TGF-β content stored in the bone volume and $\tilde{D}_{\mathrm{TGF}\text{-}\beta}$ is a constant degradation rate. $S_{\mathrm{TGF}\text{-}\beta}$ is a source/sink term for TGF-β. Note that the rate of TGF-β released from the bone matrix is assumed to be constant. In general, this release rate can be a function of space and time. Moreover, binding of TGF-β to its receptors is assumed to be much faster than changes in active osteoclast numbers. Using a quasi-steady state assumption in Eq. (10) we can express the TGF-β concentration as:

$$\mathrm{TGF}-\beta = \frac{\alpha\cdot k_{\mathrm{res}}\mathrm{OC}_{\mathrm{a}} + S_{\mathrm{TGF}-\beta}}{\tilde{D}_{\mathrm{TGF}-\beta}} \tag{11}$$

The activator and repressor functions related to TGF-β binding to its receptors can be obtained by inserting Eq. (11) into Eqs. (2) and (3). With these functions the three effects of TGF-β binding exerted on bone cells can be expressed as:

$$D_{\mathrm{OB_u}}\cdot\pi^{\mathrm{TGF}-\beta}_{\mathrm{act,OB_u}} = D_{\mathrm{OB_u}}\cdot\frac{\mathrm{TGF}-\beta}{K_{D1,\,\mathrm{TGF}-\beta}+\mathrm{TGF}-\beta} \tag{12}$$

$$D_{\mathrm{OB_p}}\cdot\mathrm{OB_p}\cdot\pi^{\mathrm{TGF}-\beta}_{\mathrm{rep,OB_p}} = D_{\mathrm{OB_p}}\cdot\mathrm{OB_p}\cdot\frac{1}{1+(\mathrm{TGF}-\beta/K_{D2,\,\mathrm{TGF}-\beta})} \tag{13}$$

$$A_{\mathrm{OC_a}}\cdot\mathrm{OC_a}\cdot\pi^{\mathrm{TGF}-\beta}_{\mathrm{act,OC_a}} = A_{\mathrm{OC_a}}\cdot\mathrm{OC_a}\cdot\frac{\mathrm{TGF}-\beta}{K_{D3,\,\mathrm{TGF}-\beta}+\mathrm{TGF}-\beta} \tag{14}$$

where $K_{D1,\mathrm{TGF}\text{-}\beta}$, $K_{D2,\mathrm{TGF}\text{-}\beta}$, and $K_{D3,\mathrm{TGF}\text{-}\beta}$ are activation/repression coefficients related to the action of TGF-β binding to its receptors expressed on osteoblasts and osteoclasts. With these terms the changes of bone cells over time related to action of TGF-β in Eqs. (4)–(6) are completely defined. The various ligand–receptor interactions and activator/repressor functions described here are summarized in Table 1.

Modeling the RANK–RANKL–OPG pathway including catabolic action of PTH

In this section the model describing the RANK–RANKL–OPG pathway including the action of PTH on RANKL and OPG expression on osteoblasts is discussed. The RANK–RANKL–OPG pathway, coupled with the action of TGF-β on bone cells, constitutes the basic known regulatory network for bone remodeling, and so is included in the model (see Fig. 1). As stated in the previous section, several systemic hormones such as glucocorticoids, estrogen, PTH, and vitamin D_3, have multiple effects on bone–cell proliferation, differentiation, activation, and apoptosis rates [2]. Among these PTH is considered to be the most important acute regulator of calcium homeostasis [22]. Given the importance of PTH, we have included its action on bone cells, at least to a first approximation, into our model.

In the following we assume that all receptor–ligand binding reactions can be expressed as:

$$A + B_j \rightleftharpoons C_j \tag{15}$$

where A and B_j are two (arbitrary) reactants and C_j denotes the molecular complex formed. The index j has been introduced for cases where molecule A is involved in several (N) reactions such as RANKL which both binds to OPG and RANK, i.e., $N=2$. Note that all other ligands (B_j) are only involved in one binding reaction.[3]

[3] In Eq. (15) A and B_j generally denote ligand (in mol/volume) and receptor (in #/cell), respectively. Cells may be present at concentrations n in a representative elementary volume (REV). This allows conversion of B_j and C_j into the same dimensions as A.

Using the principle of *mass action kinetics*, the concentration balance equation for all molecules can be described by a system of ordinary differential equations of the form:

$$\frac{dA}{dt} = -\sum_{j=1}^{N} k_{j,\mathrm{f}} A \cdot B_j + \sum_{j=1}^{N} k_{j,\mathrm{r}} C_j + S_A \tag{16}$$

$$\frac{dB_j}{dt} = -k_{j,\mathrm{f}} A \cdot B_j + k_{j,\mathrm{r}} C_j + S_{B_j} \tag{17}$$

$$\frac{dC_j}{dt} = +k_{j,\mathrm{f}} A \cdot B_j - k_{j,\mathrm{r}} C_j \tag{18}$$

where $k_{j,\mathrm{f}}$ and $k_{j,\mathrm{r}}$ are the forward and reverse reaction rate constants. S_A and S_{Bj} are source or sink terms[4], which are the sum of a production term (P_A, P_{Bj}) and a degradation term (D_A, D_{Bj}), i.e.,

$$S_A = P_A + D_A \quad \text{and} \quad S_{B_j} = P_{B_j} + D_{B_j} \tag{19}$$

In the following we assume that binding reactions leading to up-regulation and down-regulation of molecules (such as PTH binding and OPG–RANKL, RANK–RANKL binding) are much faster than the cell responses. Hence for these binding reactions we assume quasi-steady states. Inserting of Eq. (18) into Eq. (16) and Eq. (17) using the steady-state assumption gives:

$$S_A = 0 \quad \text{and} \quad S_{B_j} = 0 \tag{20}$$

which can be used as definition equations to compute the concentrations of A and B_j. The production rate of A can be decomposed in an endogenous term and an external 'dosing term', while degradation of A can be assumed to be proportional to its concentration, i.e.,

$$P_A = P_{A,e}(t) + P_{A,d}(t) \tag{21}$$

$$D_A = -\tilde{D}_A A \tag{22}$$

where $\tilde{D}_A$ is a constant degradation rate of substrate A. We further assume that endogenous production is regulated (by a ligand) and that production cannot exceed a maximum level of concentration ($A_{\max}$), i.e.

$$P_{A,e}(t) = \beta_A \cdot \pi_{\mathrm{act/rep}} \cdot \left(1 - \frac{A}{A_{\max}}\right) \tag{23}$$

Inserting of Eqs. (22) and (23) into Eq. (20) gives an expression for the concentration of A:

$$A = \frac{\beta_A \cdot \pi_{\mathrm{act/rep}} + P_{A,d}(t)}{\frac{\beta_A \cdot \pi_{\mathrm{act/rep}}}{A_{\max}} + \tilde{D}_A} \tag{24}$$

In the rest of this section we utilize Eqs. (20), (23), and (24) to derive expressions for PTH, OPG, and free RANKL concentration and the associated activator/repressor functions such as $\pi_{\mathrm{act/rep}}$. Additionally, equations for expression of OPG and RANKL on different osteoblastic cell types are given. Note that the activator function for RANKL–RANK binding (Eq. (37)) is a major component of the cell population dynamics model (see Eq. (6)) governing osteoclast differentiation.

[4] "Source" and "sink" term expresses the fact whether the overall contribution adds or removes mass during a chemical reaction according to the principles of *mass action kinetics*.

PTH binding. In the present model PTH concentration is used as a regulator of OPG and RANKL production. We assume that the PTH endogenous production is constant and not further regulated i.e., $\beta_{\mathrm{PTH}} = \mathrm{const}$, i.e., $\pi^{\mathrm{PTH}}_{\mathrm{act/rep}} = 1$. Furthermore $\mathrm{PTH}_{\max} \gg \mathrm{PTH}$ and PTH binding to its receptors on osteoblast precursor cells ($\mathrm{OB_p}$) and active osteoblasts ($\mathrm{OB_a}$) is assumed to be the same (i.e., $N = 1$). Using these assumptions in Eq. (24) we can express the PTH concentration as:

$$\mathrm{PTH} = \frac{\beta_{\mathrm{PTH}} + P_{\mathrm{PTH},d}(t)}{\tilde{D}_{\mathrm{PTH}}} \tag{25}$$

where $\tilde{D}_{\mathrm{PTH}}$ is a constant PTH degradation rate. Given the PTH concentration (Eq. (25)) we can compute activator/repressor input functions (Eqs. (2) and (3)) employed for OPG and RANKL regulation on osteoblast precursor cells and active osteoblasts as:

$$\pi^{\mathrm{PTH}}_{\mathrm{act,OB_p}} = \frac{\mathrm{PTH}}{K_{D4,\mathrm{PTH}} + \mathrm{PTH}} \text{ and } \pi^{\mathrm{PTH}}_{\mathrm{act,OB_a}} = \frac{\mathrm{PTH}}{K_{D5,\mathrm{PTH}} + \mathrm{PTH}} \tag{26}$$

$$\pi^{\mathrm{PTH}}_{\mathrm{rep,OB_p}} = \frac{1}{1 + \mathrm{PTH}/K_{D6,\mathrm{PTH}}} \text{ and } \pi^{\mathrm{PTH}}_{\mathrm{rep,OB_a}} = \frac{1}{1 + \mathrm{PTH}/K_{D7,\mathrm{PTH}}} \tag{27}$$

where we assumed a Hill coefficient of one, i.e., $n = 1$. $K_{D4,\mathrm{PTH}}$ and $K_{D5,\mathrm{PTH}}$ are activation coefficients for RANKL production related to PTH binding to osteoblastic cells. $K_{D6,\mathrm{PTH}}$ and $K_{D7,\mathrm{PTH}}$ are repression coefficients for OPG production related to PTH binding to osteoblastic cells. As a first approximation we assume that the activation and repression coefficients for different osteoblastic cells are the same, i.e., $K_{D4,\mathrm{PTH}} = K_{D5,\mathrm{PTH}}$ and $K_{D6,\mathrm{PTH}} = K_{D7,\mathrm{PTH}}$ and hence having the same activator/repressor function.

Action of PTH on RANKL and OPG expression. One key difference between the current formulation and the one proposed by Lemaire et al. [1] is the investigation of the type of cells expressing RANKL and OPG. Here we assume that both OPG and RANKL may be expressed by both osteoblast precursor cells ($\mathrm{OB_p}$) and active osteoblasts ($\mathrm{OB_a}$), and investigate the functional effect of various expression patterns on the change in bone volume.

Using the fact that OPG production is down-regulated by PTH together with Eq. (23) we can express the endogenous OPG production as:

$$P_{\mathrm{OPG},e} = \left(\beta_{1,\mathrm{OPG}} \cdot \mathrm{OB_p} \cdot \pi^{\mathrm{PTH}}_{\mathrm{rep,OB_p}} + \beta_{2,\mathrm{OPG}} \cdot \mathrm{OB_a} \cdot \pi^{\mathrm{PTH}}_{\mathrm{rep,OB_a}}\right) \cdot \left(1 - \frac{\mathrm{OPG}}{\mathrm{OPG}_{\max}}\right) \tag{28}$$

where $\beta_{1,\mathrm{OPG}}$ and $\beta_{2,\mathrm{OPG}}$ are the OPG production rates of osteoblast precursor cells and active osteoblasts. If we assume that this down-regulation by PTH is the same for osteoblast precursors and active osteoblasts, i.e., $\pi^{\mathrm{PTH}}_{\mathrm{rep,OB_p}} = \pi^{\mathrm{PTH}}_{\mathrm{rep,OB_a}} = \pi^{\mathrm{PTH}}_{\mathrm{rep,OB}}$ we can simplify Eq. (28) to:

$$P_{\mathrm{OPG},e} = \left(\beta_{1,\mathrm{OPG}} \cdot \mathrm{OB_p} + \beta_{2,\mathrm{OPG}} \cdot \mathrm{OB_a}\right) \cdot \pi^{\mathrm{PTH}}_{\mathrm{rep,OB}} \cdot \left(1 - \frac{\mathrm{OPG}}{\mathrm{OPG}_{\max}}\right) \tag{29}$$

Use of Eq. (29) in Eq. (24) we can express the OPG concentration as:

$$\mathrm{OPG} = \frac{\left(\beta_{1,\mathrm{OPG}} \cdot \mathrm{OB_p} + \beta_{2,\mathrm{OPG}} \cdot \mathrm{OB_a}\right) \cdot \pi^{\mathrm{PTH}}_{\mathrm{rep,OB}} + P_{\mathrm{OPG},d}(t)}{\frac{\left(\beta_{1,\mathrm{OPG}} \cdot \mathrm{OB_p} + \beta_{2,\mathrm{OPG}} \cdot \mathrm{OB_a}\right) \cdot \pi^{\mathrm{PTH}}_{\mathrm{rep,OB}}}{\mathrm{OPG}_{\max}} + \tilde{D}_{\mathrm{OPG}}} \tag{30}$$

Note that when $\mathrm{OPG}_{\max} \to \infty$ and $\beta_{2,\mathrm{OPG}} = 0$ then Eq. (30) and the expression for OPG proposed by Lemaire et al. [1] become identical.

RANKL is considered here a membrane bound ligand at osteoblast surfaces. The RANKL carrying capacity ($\mathrm{RANKL_{tot}}$) on osteoblast surfaces must be restricted by an upper limit, which can never be exceeded. This so-called 'effective carrying capacity' ($\mathrm{RANKL_{eff}}$) which is the maximum concentration of RANKL, is assumed to be regulated by PTH and may be express as:

$$\begin{aligned} \mathrm{RANKL_{eff}} &= \mathrm{RANKL_{OB_p,eff}} + \mathrm{RANKL_{OB_a,eff}} \\ &= \left(R_1^{\mathrm{RANKL}} \cdot \mathrm{OB_p} + R_2^{\mathrm{RANKL}} \cdot \mathrm{OB_a}\right) \cdot \pi^{\mathrm{PTH}}_{\mathrm{act,OB}} \end{aligned} \tag{31}$$

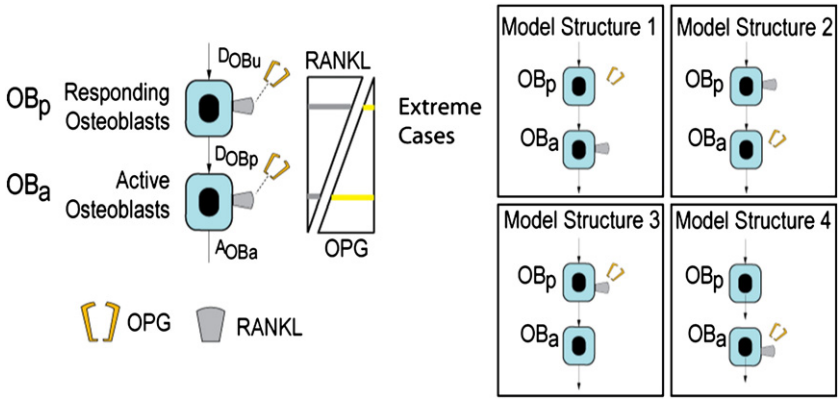

Fig. 2. Biologically observed expression of OPG and RANKL on osteoblastic cells and derived extreme cases: (a) Model structure 1, (b) Model structure 2, (c) Model structure 3, and (d) Model structure 4.

where we again assume that up-regulation by PTH is the same for osteoblast precursor cells and active osteoblasts, i.e., $\pi^{PTH}_{act,OB_p} = \pi^{PTH}_{act,OB_a} = \pi^{PTH}_{act,OB}$. The constants R^{RANKL}_1 and R^{RANKL}_2 are the maximum number of RANKL (receptors) on osteoblast precursor cells and active osteoblasts. The total concentration of RANKL at any time is the sum of free RANKL and RANKL complexes, i.e.,

$$\begin{aligned} \mathrm{RANKL_{tot}} &= \mathrm{RANKL} + [\mathrm{RANKL} - \mathrm{OPG}] + [\mathrm{RANKL} - \mathrm{RANK}] \\ &= \mathrm{RANKL} \cdot (1 + K_{A1,\mathrm{RANKL}} \cdot \mathrm{OPG} + K_{A2,\mathrm{RANKL}} \cdot \mathrm{RANK}) \end{aligned} \tag{32}$$

where use of the steady-state expressions for complexes was made. $K_{A1,\mathrm{RANKL}}$ and $K_{A2,\mathrm{RANKL}}$ are the association binding constants of RANKL to OPG and RANK respectively (see Table 3). With the definitions above we can formulate production and degradation rate of RANKL as follows:

$$P_{\mathrm{RANKL}} = P_{\mathrm{RANKL},e} + P_{\mathrm{RANKL},d} \tag{33}$$

$$P_{\mathrm{RANKL},e} = \beta_{\mathrm{RANKL}} \left(1 - \frac{\mathrm{RANKL_{tot}}}{\mathrm{RANKL_{eff}}}\right) \tag{34}$$

$$D_{\mathrm{RANKL}} = -\tilde{D}_{\mathrm{RANKL}} \cdot \mathrm{RANKL_{tot}} \tag{35}$$

where $P_{\mathrm{RANKL},e}$ and $P_{\mathrm{RANKL},d}$ is the endogenous RANKL production rate and external dosing rate respectively. β_{RANKL} and $\tilde{D}_{\mathrm{RANKL}}$ is the RANKL production and degradation rate.

Using the steady-state condition (Eq. (19)) $P_{\mathrm{RANKL}} + D_{\mathrm{RANKL}} = 0$ we can express the RANKL concentration as:

$$\mathrm{RANKL} = \frac{\mathrm{RANKL_{eff}}}{1 + K_{A1,\mathrm{RANKL}}\mathrm{OPG} + K_{A2,\mathrm{RANKL}}\mathrm{RANK}} \left(\frac{\beta_{\mathrm{RANKL},1} + P_{\mathrm{RANKL},d}}{\beta_{\mathrm{RANKL}} + \tilde{D}_{\mathrm{RANKL}}\mathrm{RANKL_{eff}}} \right) \tag{36}$$

With the definition of free RANKL concentration (i.e. Eq. (36)), we can now formulate a Hill activator function (Eqn.(2)) which regulates differentiation of osteoclast precursor cells:

$$\pi^{\mathrm{RANKL}}_{act,OC_p} = \frac{\mathrm{RANKL}}{K_{D8,\mathrm{RANKL}} + \mathrm{RANKL}} \tag{37}$$

where $K_{D8,\mathrm{RANKL}}$ is the activation coefficient related to RANKL binding to RANK. The RANKL activator function (Eq. (37)) controls differentiation of osteoclast precursor cells into active osteoclasts (see Eq. (6)).

The various molecules (i.e., ligands, receptors and complexes) and associated activator/repressor functions considered in the model are summarized in Table 1.

Numerical investigation of bone remodeling by BMUs

Bone remodeling is an important mechanism to repair microdamage due to cyclic loading during daily activities such as walking, running etc. This repair process is executed by bone cells such as osteoblasts and osteoclasts, which are tightly coupled through the RANK–RANKL–OPG system, together with the action of TGF-β on bone cells. Osteoblasts and osteoclasts work together in so-called basic multicellular units (BMUs). BMUs react very sensitively to any changes of the bone microenvironment. Consequently, modification of any of its components is expected to have significant effects on bone turnover and homeostasis. Here we specifically consider the effect of expressing RANKL and OPG on different cell types in the osteoblastic cell lineage (here referred to the 'expression profile'). Using our selection criterion for the 'optimal model structure' as the one having the 'maximum effect' on bone volume change, we seek to find a preferred arrangement for ligand expression on particular cell types.

Once an optimum arrangement of ligand expression is found (see Effects of model structure on bone remodeling), we perform an extensive parametric study investigating model parameters related to cell differentiation and apoptosis.[5] Using tools of computational systems biology, we identify putative control mechanisms for physiologically reasonable bone remodeling responses (see Identification of control mechanisms for bone remodeling).

Effects of model structure on bone remodeling

Here we consider an important aspect of model structure i.e. expression of RANKL and OPG on different cell types in the maturing osteoblastic cell lineage (see Fig. 2). Several bone biology research groups have identified the importance of RANKL and OPG expression on maturing osteoblastic cells [36,37,42–44]. Summarizing these research findings, RANKL concentration is high on osteoblast precursor cells while low on active osteoblasts. On the other hand, the opposite holds for OPG production. We suspect that this particular ligand/decoy receptor expression structure is not accidental, and is more than likely important in the coordination of cells into a functional BMU.

Therefore, in the following we investigate four extreme cases related to expression of RANKL and OPG (see Fig. 2): *Model structure 1* — RANKL is expressed on OB_a, while OPG is expressed on OB_p (this is the model structure adopted in the Lemaire et al. model),

[5] In all numerical simulations the number of RANK receptors on OC_p's is assumed to be constant — this assumption may be relaxed in a future study.

Table 2
Expression of RANKL/OPG on osteoblastic cells

Model structure	Osteoplast precursor — OB_p		Active osteoblast — OB_a	
	RANKL	OPG	RANKL	OPG
MS1	0	1	1	0
MS2	1	0	0	1
MS3	1	1	0	0
MS4	0	0	1	1

(0 … no expression; 1 … fully expressed; all model structures are scaled to MS1, i.e., MS2: $0\times\beta_{1,OPG}(MS1)\times OB_{a,t0}(MS1)/OB_{p,t_0}(MS1)$, $1\times\beta_{2,OPG}(MS1)\times OB_{a,t0}(MS1)/OB_{p,t0}(MS1)$, $1\times R_1^{RANKL}\times OB_{a,t0}(MS1)/OB_{p,t0}(MS1)$, $0\times R_2^{RANKL}\times OB_{a,t0}(MS1)/OB_{p,t0}(MS1)$).

Model structure 2 — RANKL is expressed on OB_p, while OPG is expressed on OB_a (this is the model structure reported by several research groups [36,37,42]), *Model structure 3* — RANKL and OPG are both expressed only on OB_p, and *Model structure 4* — RANKL and OPG are both expressed only on OB_a. These four structures can be obtained by specifying the expression parameters of OPG and RANKL in Eqs. (30) and (36). A summary of these four model structures to be investigated, together with model parameters employed in each structure, is shown in Table 2.

The effect of the four model structures can be investigated by first defining an objective criterion for the assessment of each model structure. Here we have chosen the objective criterion as the sensitivity of the four model structures, where sensitivity is here defined as the responsiveness of bone volume (BV)[6] to 'system perturbations'. The system perturbations can potentially take any form, from changes in differentiation rates, to injection of cells or changes of PTH concentration, but here we only consider changes in differentiation and apoptosis rates of different cell types, as these are the fundamental cell lineage behaviours.

As different model structures lead to different RANKL/OPG ratios and hence, to different steady-state cell numbers, the expression constants of RANKL and OPG in Eqs. (30) and (36) need to be calibrated such that the steady-state cell numbers are the same for all model structures. This was implemented by multiplying the steady-state cell number ratio of OB_a to OB_p from Model structure 1, to other cases whose receptor configuration differed from Model structure 1. For example in Model structure 2 both RANKL and OPG were modified as both receptors had a different configuration to Model structure 1 (see Table 2 for details).

Once this model calibration has been performed, a change in cell differentiation or apoptosis rate is applied for a period of 100 days, and then removed in order for the system to settle towards a steady state (over another 100 days). Changes of any system parameter lead to changes of bone volume (which results from the integrated effects of cell numbers over time). Fig. 3 shows schematically typical bone volume vs. time curves for a change of a system parameter leading to an initial increase of osteoclast numbers. In this figure three characteristic model outputs can be identified: (1) bone volume loss, (2) no change in bone volume, and (3) bone volume gain. Depending on the dynamic properties of the system and the imposed change, one of these outcomes will be obtained.

In the first example, we investigate an increase of the differentiation rate D_{OCp} of osteoclast precursor cells (the applied increase is a factor of 10, which leads to an increase of active osteoclasts). Fig. 4 shows the change of bone volume for this

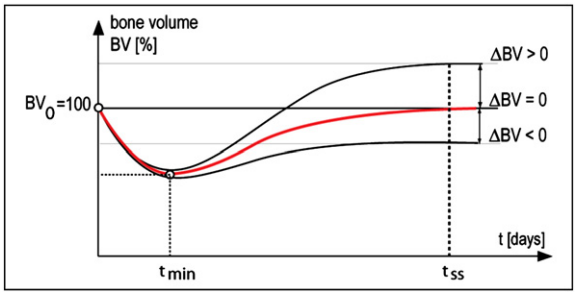

Fig. 3. Schematic illustration of bone volume [%] vs. time [days] curves leading to different overall changes of bone volume (based on perturbation of steady state leading to increased osteoclast activity).

system perturbation vs. time for the four Model structures, indicating that an increase of D_{OCp} over 100 days leads to overall bone loss. Comparison of bone volume vs. time plots for the different model structures indicates that Model structure 2 (full line in Fig. 4) leads to a much larger change in bone volume for the same change of differentiation rate of osteoclast precursor cells, i.e. a change of D_{OCp}, relative to other model structures. The same behaviour is obtained for the bone turnover (OC_a+OB_a) curves, though these are not shown here.

The different bone volume vs. time curves are best explained by looking at changes of free RANKL concentration over time for different model structures (see Fig. 5a). Fig. 5a indicates that the RANKL concentration strongly increases for Model structure 2, while it decreases for Model structure 1. Values for the two remaining model structures are in between these upper and lower bound of RANKL concentration. An increase in RANKL concentration leads to an increase of the RANK receptor occupancy (π^{RANKL}_{act,OC_p}) on osteoclast precursor cells and, hence, to increases in active osteoclast numbers. This leads to a net bone resorption. Comparing how different bone cells are affected by the choice of model structure, one can see that differences in the active osteoclast numbers are most pronounced at $t=100$ days followed by OB_p's and OB_a's. At $t=200$ days these differences in cell numbers can still be observed, however, these differences are not as pronounced.

These results suggest that Model structure 2 is the 'optimal' ligand expression, because it is this particular ligand configuration which is most responsive to a change in D_{OCp}, and so offers the

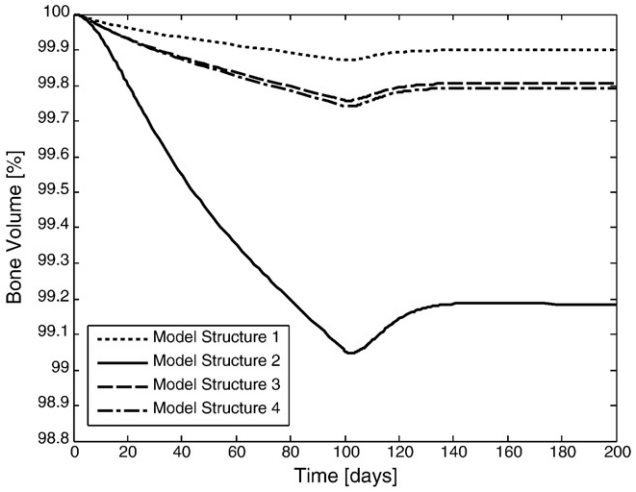

Fig. 4. Bone volume [%] vs. time [days] curves obtained for Model Structures 1 to 4 for an increase of osteoclast differentiation rate of $D_{OCp}=e\times D_{OCp0}$ (e…Euler number).

[6] It is noted that we actually investigated several objective functions including bone volume, bone turnover (i.e., overall cell numbers) and the ratio of active cells (OC_a/OB_a). However, for a more concise discussion of results we chose to only use bone volume as an objective criterion.

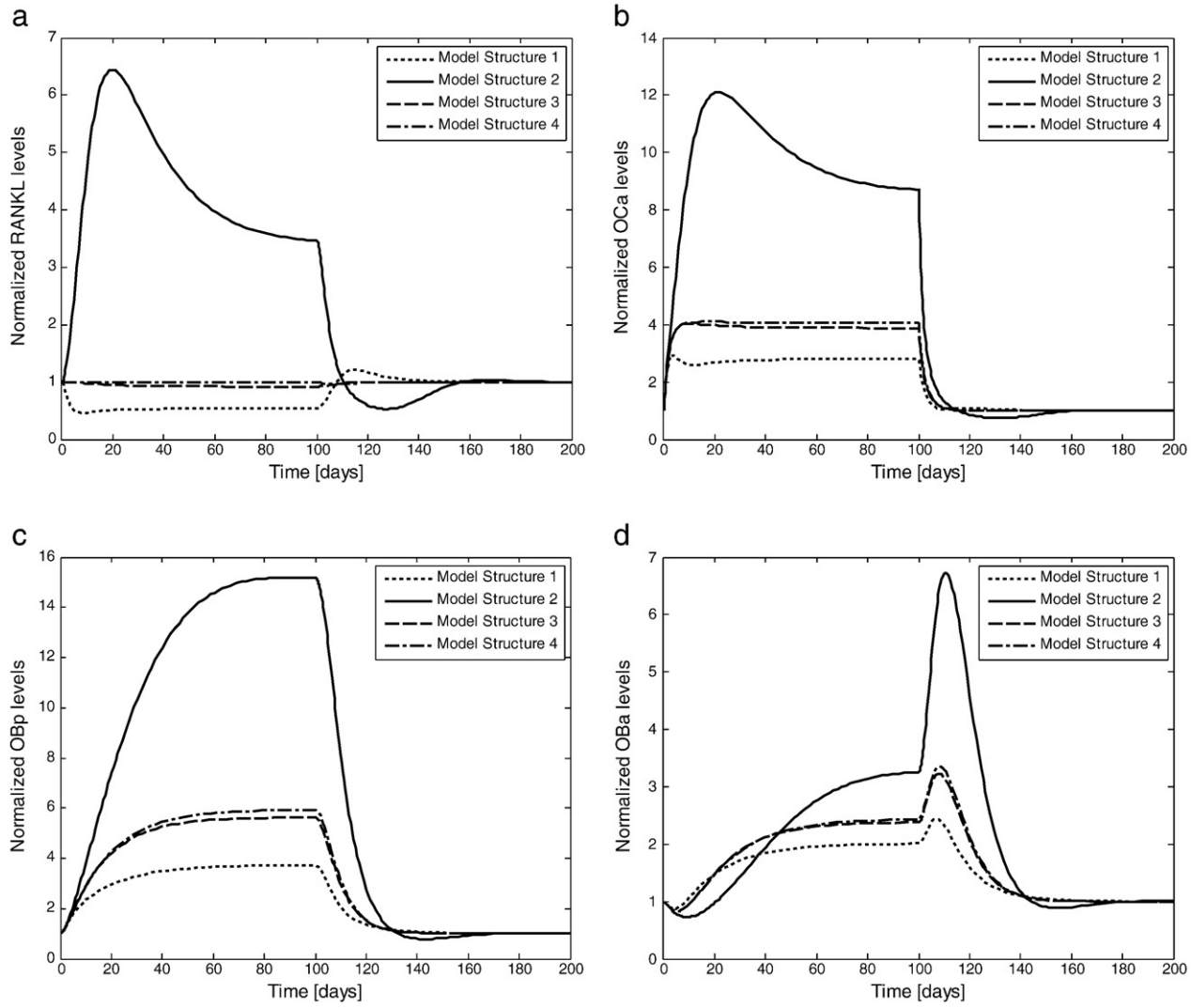

Fig. 5. Normalized plots of RANKL and bone–cell concentration vs. time [days] for Model Structures 1 to 4 for an increase of osteoclast differentiation rate ($D_{OCp}=e\times D_{OCp0}$): (a) free RANKL, (b) OC_a, (c) OB_p and (d) OB_a.

greatest functional effect of the BMU on bone volume, and so the greatest potential for an effective functional control of the bone volume.

To confirm this initial hypothesis as to the optimal model structure, we now investigate system behaviour for a wide range of changes of differentiation and apoptosis rates of osteoblastic and osteoclastic cells. In order to do this, we have applied exponentially differing 'multiplication factors' (i.e., 10^p) to each differentiation and apoptosis rate, for five differentiation/apoptosis rate parameters in total. This multiplication factor has been varied from by 10 orders of magnitude, i.e., exponent $p=-5$ to $p=5$ in step intervals of 0.25, and so covers a wide range of model parameters. The time dependent (output) function for bone volume is sampled at 100 days and 200 days to represent the maximal change and a later change in bone volume, following removal of the stimulus. However as both time instants deliver qualitatively similar findings, only the day 100 bone volume change results are reported. Figs. 6a–e represent the influence of parameter variations on the numerical results.

In order to concisely represent the large amount of numerical data, all cell numbers have been normalized with respect to the initial steady-state cell numbers. RANKL concentration was normalized with respect to the initial steady-state RANKL concentration. For most effective representation of data, ordinates of bone volume curves have been restricted to ±2.5% and four orders of magnitude variation, i.e., exponent $p=-2$ to $p=2$.

Comparison of the bone volume curves for different values of model parameters (Fig. 6) indicates that Model structure 2 delivers the most significant effect on bone volume (BV) for a given perturbation compared to the other model structures with the only exception of decreasing A_{OBa}. The effect is most pronounced for changes of D_{OCp} and D_{OBu} which lead to an exponential change in bone volume, i.e., decreasing BV with increasing D_{OCp} and increasing BV for increasing D_{OBu}. Changes of other model parameters such as e.g. A_{OCa} have a moderate effect on the bone volume. These results confirm the above hypothesis that Model structure 2 is the most sensitive model structure.

It is noted that the observed exponential increases and decreases of bone volume above are likely to be associated with very large changes of parameter values, which may be be non-physiological. Unfortunately, currently available experimental data on cell numbers is only available from histomorphometric studies and hence provide only limited information on cell numbers.

Taking into account the physiological limits of the system response, we observe that in all cases (but one) shown above Model structure 2 is the most sensitive to changes in model parameters. Biologically, this

sensitivity is desirable because the BMU is most functionally responsive, and so in this configuration bone cells can most effectively respond to any changes of the microenvironment. Hence, the model results suggest that Model structure 2 is the functionally expected expression pattern of OPG/RANKL on osteoblastic cells. This is confirmed by biological observations [36,37,42–44].

For these reasons we identify Model structure 2 as the optimal ligand expression pattern that leads to the most functionally effective BMU. We note here that the findings presented in this paper contrasts with the OPG/RANKL expression pattern assumed in the Lemaire et al. [1] paper. In fact, this expression pattern is identified as least functionally effective.

So far we have identified an optimal ligand configuration. However based on the parametric study on changes of individual differentiation/apoptosis rates presented above, no clear method for controlling bone volume changes has been found. This is the subject of the next section.

Identification of control mechanisms for bone remodeling

The parametric study presented above indicates that variation of some model parameters either give rise to physiologically unrealistic large changes in bone volume, while others lead to hardly any changes in bone volume. From a control theory viewpoint,

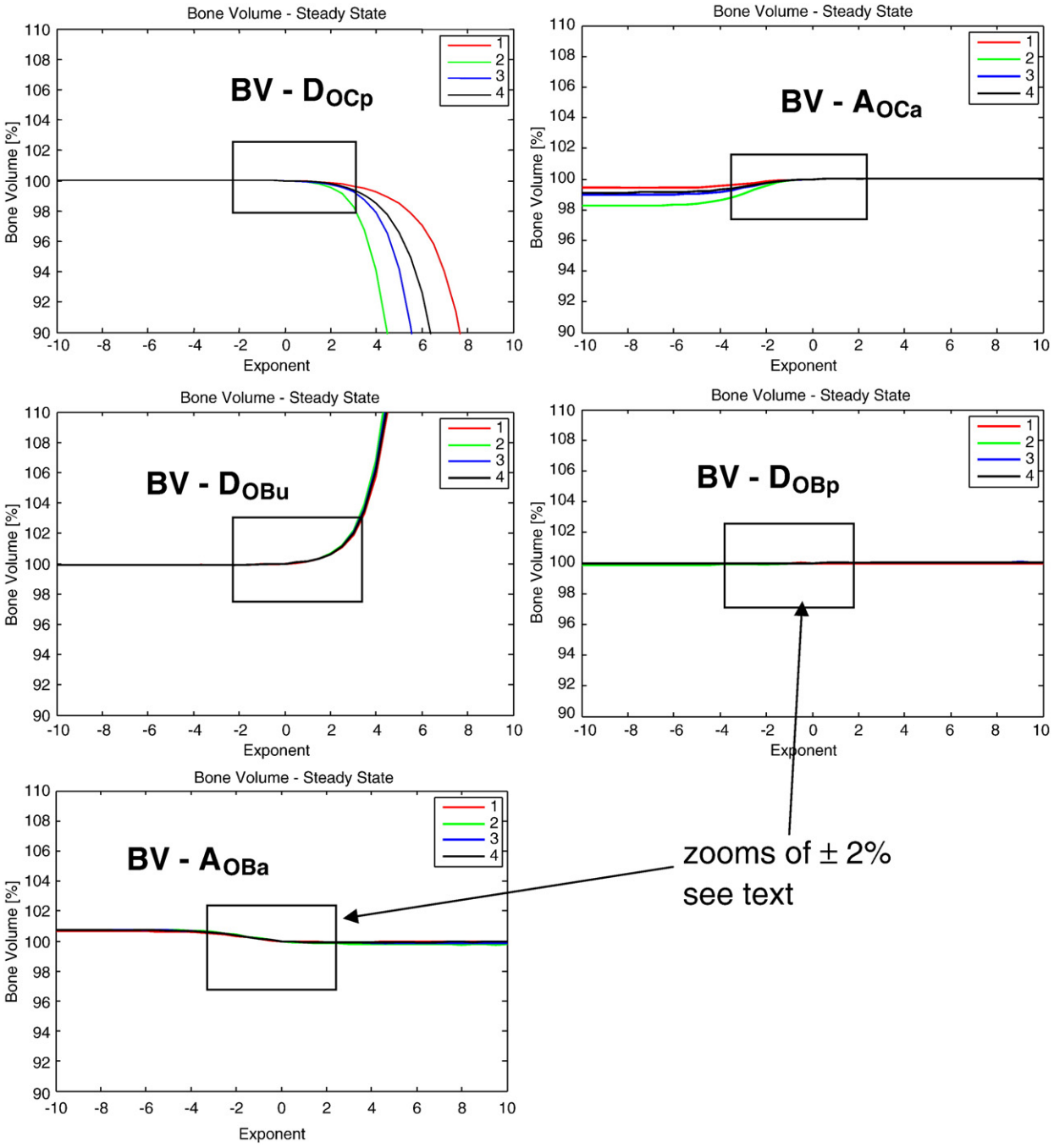

Fig. 6. Bone volume [%] vs. changes of model parameters "$[e^{-10}$–$e^{+10}]\times p$": (a) D_{OCp}; (b) A_{OCa}; (c) D_{OBu}; (d) D_{OBp}; (e) A_{OBa} (evaluated at t=60 days; e…Euler number).

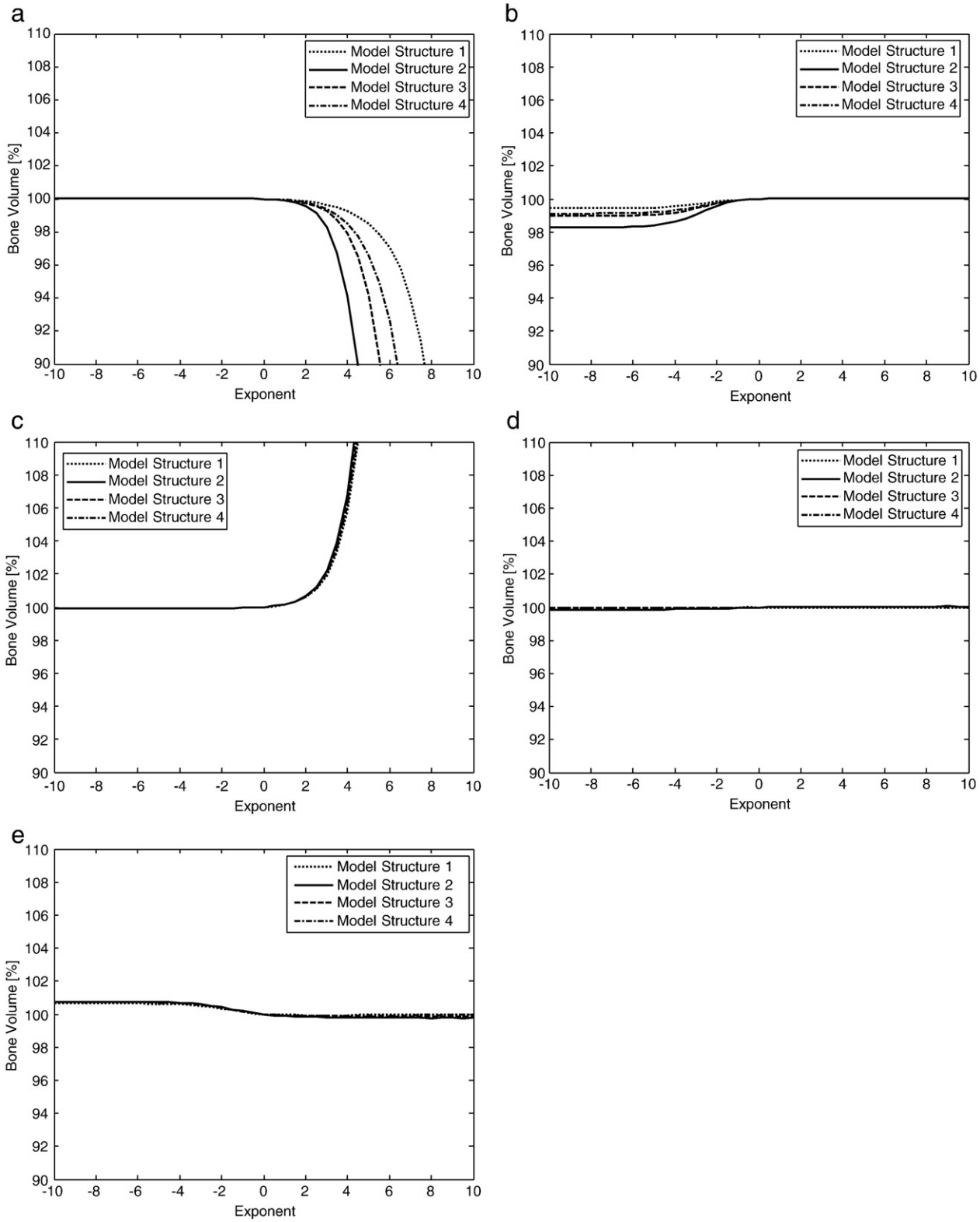

Fig. 6 (*continued*).

one can argue that a complex system such as the bone remodeling unit (BMU) would have several control mechanisms acting simultaneously, i.e., a BMU's response to changes in bone microenvironment would be governed by a simultaneous change in differentiation/apoptosis rates of bone cells. In order to investigate such a scenario we now perform simultaneous combinations of change of two or more differentiation/apoptosis rates, with the aim to find an "optimal" parameter combination which allows the BMU to respond in a controlled way to applied changes in differentiation/apoptosis rates.

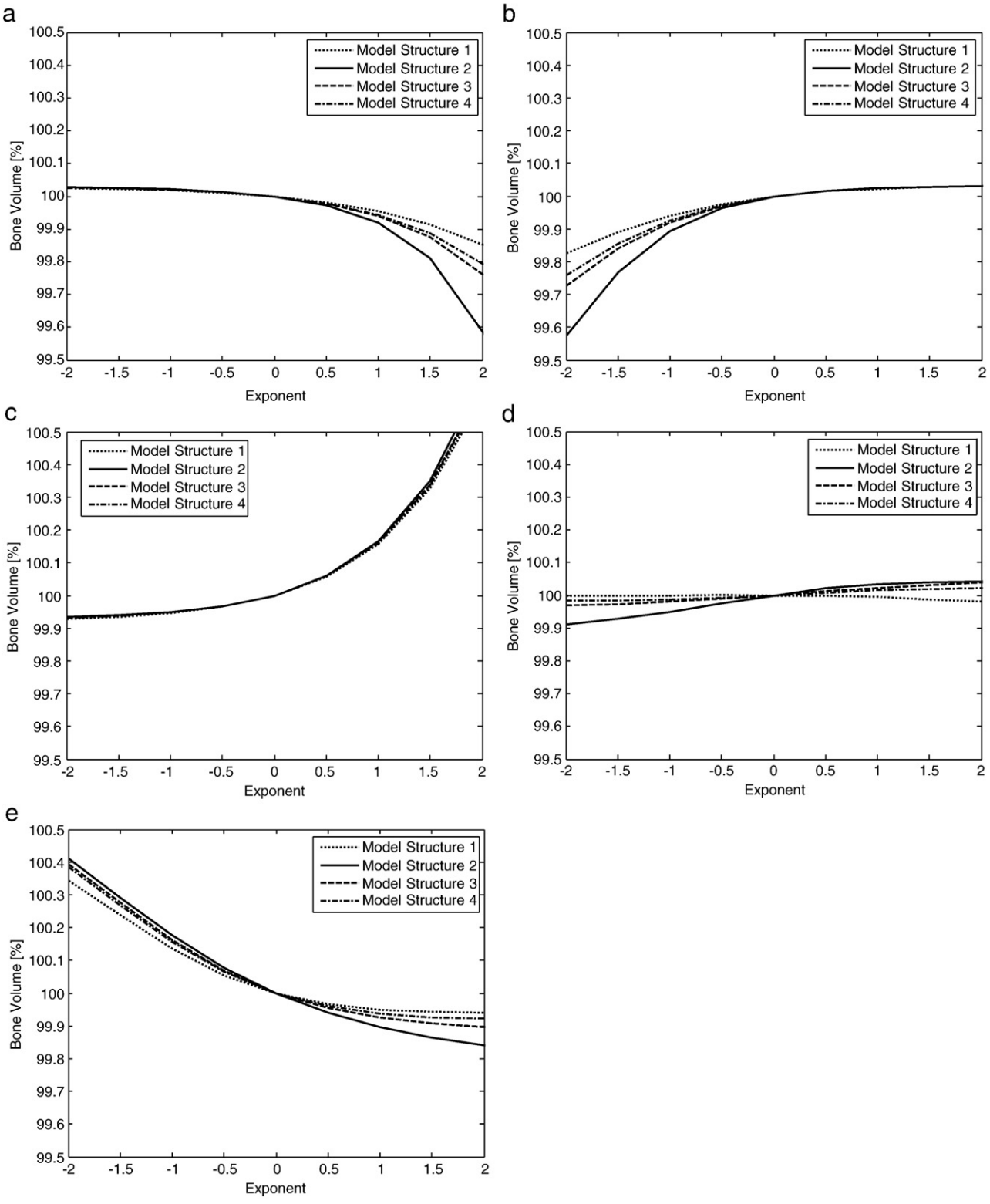

Fig. 6 (*continued*).

In the following simulations we work with Model structure 2 (i.e. RANKL expressed on responding osteoblasts, and OPG expressed on active osteoblasts), and search the model parameter space for combinations of changes in differentiation and apoptosis rates, noting their effects on changing bone volume.

The parameter space consists of five parameters (D_{OCp}, A_{OCa}, D_{OBu}, D_{OBp}, A_{OBa}) as described in Effects of model structure on bone remodeling. We vary parameter perturbations up and down in groups of first two, then three, then four, and finally five at a time. This gives ${}^{n}C_{k}$ combinations, i.e., ${}^{5}C_{2}$, ${}^{5}C_{3}$, ${}^{5}C_{4}$, ${}^{5}C_{5}$, each with 10, 10, 5, 1

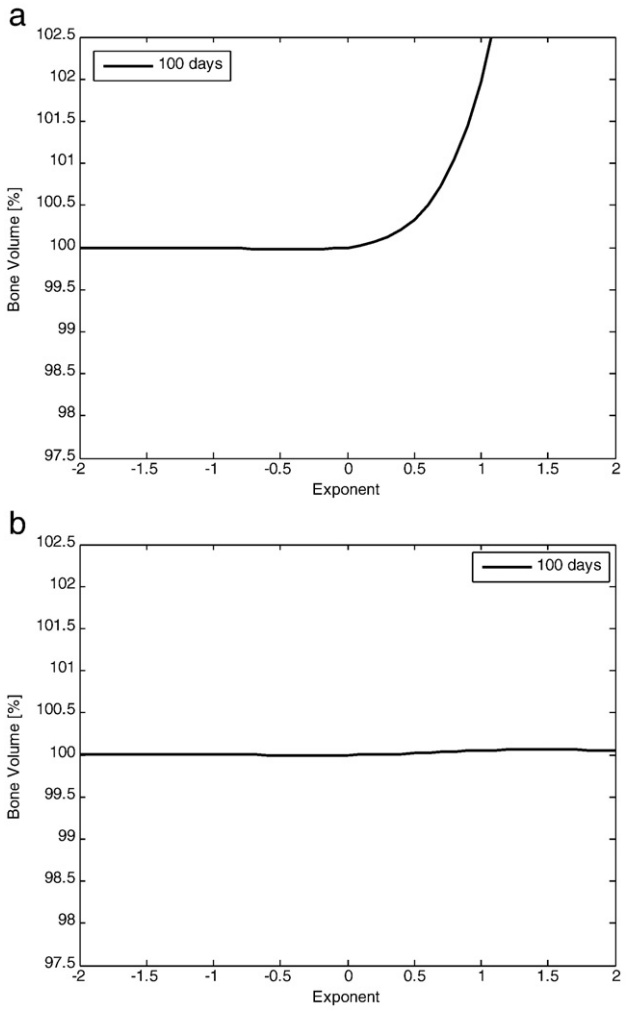

Fig. 7. Physiological unrealistic changes of bone volume vs. combined changes of model parameter "[e^{-10}–e^{+10}]·p": (a) exponential bone growth for D_{OCp}/D_{OBu}=+/+ and (b) small changes of ΔBV for entire parameter space — $D_{OCp}/A_{OCa}/D_{OBp}$=−/−/− (evaluated at t=120 days; e…Euler number; p…parameter value).

combinations, respectively. As for each of these cases, the parameters may be up or down-regulated, this leads to k^2 permutations.[7] This leads to ${}^nC_k \cdot k^2$ permutations in total, that is 232 possible permutations are simulated (i.e. 40, 80, 80, and 32 permutations for variations of differentiations rates 2, 3, 4 and 5 at a time respectively). The response curves are defined as BV change at 100 days vs. change in model parameters. Note that the system perturbations have been applied in the same way as in *Effects of model structure on bone remodeling*. Among these 232 response curves, a subset of generic response curves could be identified, which accounts for general system behaviour. This is discussed in the following paragraph.

Fig. 7 summarizes two generic response curves representing physiological unrealistic behaviour. The first type of response curve exhibits 'exponential behaviour' (as indicated in Fig. 7a which shows an exponential growth of bone volume ΔBV for increasing the differentiation rates of osteoblast progenitor cells and osteoblast precursor cells, i.e., D_{OBu}/D_{OBp}=+/+). This type of behaviour was obtained for a quite large range of model parameter combinations. From a biological point of view, such an unbounded exponential change in bone volume (ΔBV) is physiologically dangerous (leading to osteopetrosis), and does not represent a realistic control mechanism. For processes leading to parameter combinations giving an exponential response in bone volume, the system clearly is unable to respond in a stable (i.e. bounded) way. Hence, all model parameter combinations leading to this type of bone volume change are excluded from further analysis here.

At the other extreme, Fig. 7b shows only slight changes of bone volume (ΔBV) for the selected choice of model parameters changes (i.e. the curves are very flat), over the entire range of parameter change. Again many parameter permutations could be identified leading to response curves of this type. All these parameter permutations are excluded on the grounds they do not provide an effective control mechanism for regulating bone volume by BMUs.

Having now identified those parameter combinations which do not allow for effective control of bone volume, we want to briefly discuss what might be expected as an 'ideal' regulatory response by functionally active BMUs. A normal bone remodeling cycle is characterized by the same amount of resorption to formation and, hence, by zero changes in bone volume (ΔBV=0). In this state we can identify typical concentrations of hormones, growth factors, cytokines, etc. which lead to the 'normal' (i.e., reference) differentiation/apoptosis rates in BMUs. In order to account for slight fluctuations in concentrations one would expect BMUs to be rather insensitive to these changes — hence one may identify a region around the usual operating state of BMUs with relatively small gradients of changes in bone volume in response to changes in differentiation rates, with larger gradients for larger changes in differentiation rates. However, if the differentiation rates increase significantly, one would expect to see this response in bone volume change to remain bounded. For the bone volume to increase indefinitely is physiologically unrealistic. Further, if the differentiation rates decrease significantly, one would expect that the rate of bone volume change would decrease, but again this decrease should also be bounded. In fact physiologically it makes sense for the bone volume change to become zero for very low differentiation rates. This 'ideal behaviour' is schematically illustrated in Fig. 8. In this figure we can identify point A as the threshold concentration — any change of model parameter below A does not lead to changes in bone volume. Point F marks the maximum concentration which leads to the maximum change in bone volume (ΔBV_{max}), any further increase of concentration does not lead to further bone formation. Around the steady-state (reference) configuration (point D) we can identify a region (C–D and D–E) characterized by small gradients of ΔBV — indicating insensitivity to small fluctuations in model parameters. As parameter values exceed this range, larger changes of bone volume are obtained — indicating that BMUs are functionally responsive to changes in model parameters. As we identified a minimum concentration (point A) which does not lead to further changes of bone volume there must be a transition regime

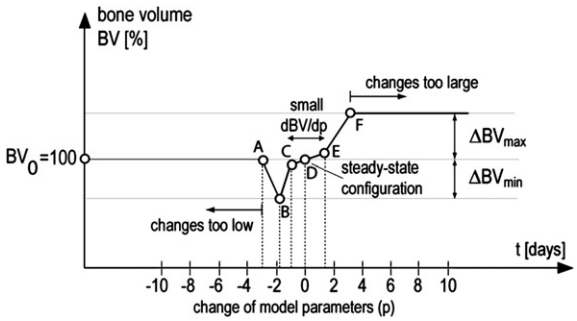

Fig. 8. Schematic illustration of ideal response curve (i.e., change of bone volume envelope) for combined changes in model parameters.

[7] Note that increases or decreases in each model parameter are made by a fixed amount, i.e., each differentiation/apoptosis rate is only increased or decreased by *p%*. For example changes in A_{OBa}, D_{OBp}, could be up-regulated while A_{OBa} could be down regulated which may be expressed as "+/+/-".

from point C to A which is characterized by a decrease of bone volume with decreasing concentration.

Having identified a potential 'ideal response envelope', we can now look for response curves that may fit these idealised requirements. Most pleasingly, we have been able to identify a small subset of curves that are similar to the idealised response curve. Parameter combinations leading to idealized response curves are given in Table 4. Among these combinations there are two categories of response curves – one which gives almost the same response curves for $t=100$ days and $t=200$ days; the other one giving two different curves. In the latter category we have identified two parameter combinations, i.e., a parameter permutation involving three parameters ($D_{OBu}/D_{OBp}/A_{Oca}=+/-/+$), and the other combination arising from a permutation involving four parameters ($D_{OBu}/D_{OBp}/A_{OBa}/A_{OCa}=+/-/-/+$). The response curves are shown in Fig. 9. These curves, especially the latter, show a close similarity to the idealised response curve shown in Fig. 8.

Most interestingly, it turns out that the curve involving three parameters coincides with the known physiological action of TGF-β on bone cells. TGF-β promotes differentiation of osteoblast progenitors, inhibits differentiation of osteoblast precursor cells; while promoting of osteoclast apoptosis (i.e., $D_{OBu}/D_{OBp}/A_{OCa}=+/-/+$). In other words, we appear to have found a physiologically plausible explanation for the known physiological actions of TGF-β in bone i.e. TGF-β leads to a response curve for bone volume change that is functionally sensible.

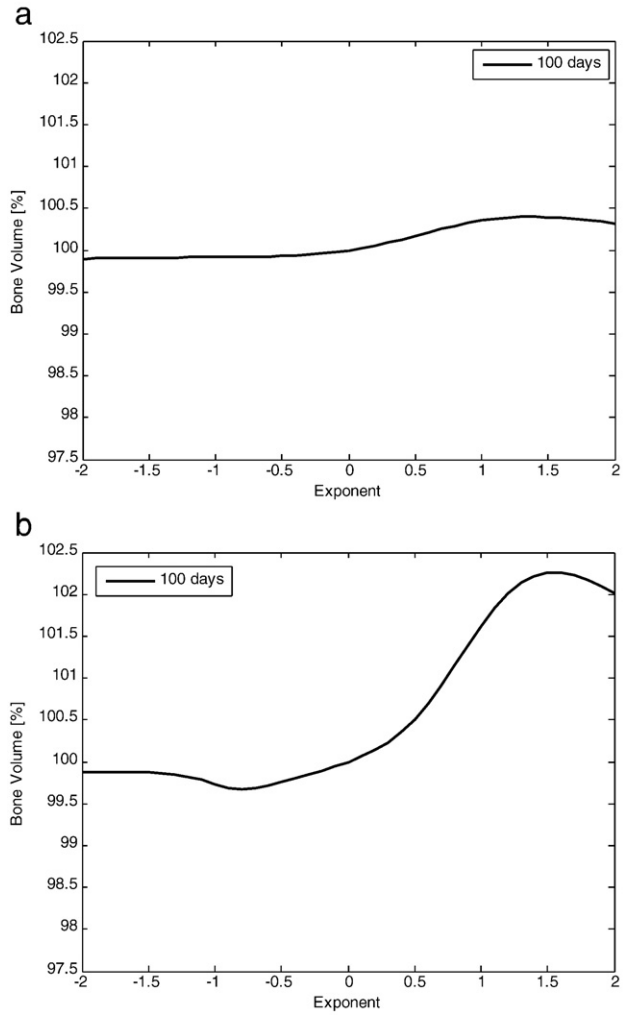

Fig. 9. Physiological realistic changes of bone volume vs. combined changes of model parameter values: (a) $D_{OBu}/D_{OBp}/A_{OCa}=+/-/+$ and (b) $D_{OBu}/D_{OBp}/A_{OBa}/A_{OCa}=+/-/-/+$ (evaluated at $t=120$ days).

Table 3
Model parameters used for bone–cell dynamic model

Bone–cell dynamic model			
Symbol	Value	Unit	Description
D_{OB_u}	7.000×10^{-4}	[pM OB_u]/day	Differentiation rate of OB progenitors
D_{OB_p}	5.348×10^{0}	[pM OB_p]/day	Differentiation rate of responding OB
A_{Ob_a}	1.890×10^{-1}	[pM OB_a]/day	Rate of elimination of active OB
D_{Oc_p}	2.100×10^{-3}	[pM OC_p]/day	Rate of elimination of active OB
A_{Oc_a}	7.000×10^{-1}	[pM OC_a]/day	Rate of OC apoptosis caused by TGF-β
$K_{D1,TGF-\beta}$, $K_{D3,TGF-\beta}$	4.545×10^{-3}	[pM]	Activation coefficients related to TGF-β binding on OB_u and OC_a
$K_{D2,TGF-\beta}$	1.416×10^{-3}	[pM]	Repression coefficients related to TGF-β binding on OB_p
$K_{D4,PTH}$, $K_{D5,PTH}$	1.500×10^{2}	[pM]	Activation coefficient for RANKL production related to PTH binding
$K_{D6,PTH}$, $K_{D7,PTH}$	2.226×10^{-1}	[pM]	Activation coefficient for RANK production related to RANKL binding
$K_{D8,RANKL}$	1.306×10^{1}	[pM]	Activation coefficient related to RANKL binding to RANK
RANK	1.000×10^{1}	[pM]	Fixed concentration of RANK
R_1^{RANKL}, R_2^{RANKL}	3.000×10^{6}	[−]	Maximum # of RANKL on each cell surface (1… OB_p, 2… OB_a); scaled to MS 1 (see Table 2)
β_{RANKL}	1.684×10^{4}	[pM RANKL]/[pm cell]	Production rate of RANKL per cell
$\tilde{D}_{RANKL}$	1.013×10^{1}	[pM RANKL]/day	Rate of degradation of RANKL
$\tilde{D}_{OPG}$	3.500×10^{-1}	[pM OPG]/day	Rate of degradation of OPG
$\beta_{1,OPG}$ $\beta_{2,OPG}$	1.464×10^{8}	[pM OPG]/[pM cell]	Minimum rate of production of OPG per cell, only for Model Structure 1; other MS are scaled accordingly (refer to Table 2)
OPG_{max}	2.000×10^{8}	pM OPG	Maximum possible OPG concentration
$K_{A1,RANKL}$	1.000×10^{-3}	[pM OPG]$^{-1}$	Association binding constant RANKL–OPG
$K_{A2,RANKL}$	3.412×10^{-2}	[pM RANKL]$^{-1}$	Association binding constant RANKL–RANK
$\tilde{D}_{PTH}$	8.600×10^{1}	[pM PTH]/day	Rate of degradation of PTH
β_{PTH}	2.500×10^{2}	[pM PTH]/day	Rate of synthesis of systematic PTH
$\tilde{D}_{TGF-\beta}$	1.000×10^{0}	[pM PTH]/day	Rate of degradation of TGF-β
α	1.000×10^{0}	[%]	TGF-β content stored in bone matrix in
K_{res}	1.000×10^{0}	[%]	Relative rate of bone resorption (normalized with respect to normal bone resorption)
K_{form}	1.571×10^{0}	[%]	Relative rate of bone formation (normalized with respect to normal bone formation)

As the second response curve involving four parameters involves three of the parameters in the first curve, one may reasonably postulate that TGF-β would have a fourth physiological action, viz, increasing the apoptosis rate of the osteoblasts. We note including this leads to a closer approximation to our idealised response curve.

Summary and conclusions

In this paper we propose a bone–cell population dynamics model describing bone remodeling events occurring in basic multicellular units (BMUs). A focus in the model formulation is the incorporation of RANKL and OPG expression on cells of the osteoblastic lineage at different stages of maturation. Although experimental data on OPG and RANKL expression of osteoblastic cells suggests that RANKL is highly expressed in osteoblast precursor cells, while OPG is highly expressed on active osteoblasts, no clear biological reason has been

Table 4
Parameter combinations of differentiation and apoptosis rates together with particular action on BMUs (see also Fig. 1) leading to controlled remodeling responses (+... parameter increase; -... parameter decrease; shaded combinations give different response curves for $t = 100$ days and $t = 200$ days; *... associated with the action of TGF-β; **... these response curves are shown in Fig. 9)

#	Combination of differentiation and apoptosis rates	Action on BMUs
2	A_{OCa}/D_{OBu}	+/+
2	A_{OCa}/A_{OBa}	−/−
2	D_{OBu}/D_{OBp}	+/−
2	D_{OBp}/A_{Oba}	+/−
3	$A_{OCa}/D_{OBu}/D_{OBp}$ *, **	+/+/−
3	$A_{OCa}/D_{OBp}/A_{OBa}$	−/+/−
3	$D_{OCp}/D_{OBu}/D_{OBp}$	+/+/−
3	$D_{OBu}/D_{OBp}/A_{OCa}$	+/−/+
3	$D_{OCp}/D_{OBp}/A_{OBa}$	+/+/−
3	$A_{OCa}/D_{OBp}/A_{OBa}$	−/+/−
4	$D_{OCp}/A_{OCa}/D_{OBu}/D_{OBp}$ *	+/+/+/−
4	$D_{OCp}/A_{OCa}/D_{OBu}/D_{OBp}$	−/+/+/−
4	$A_{OCa}/D_{OBu}/D_{OBp}/A_{OBa}$ *, **	+/+/−/−
4	$D_{OCp}/A_{OCa}/D_{OBp}/A_{OBa}$	−/−/+/−
4	$D_{OCp}/A_{OCa}/D_{OBp}/A_{OBa}$	+/−/+/−
4	$D_{OCp}/A_{OCa}/D_{OBu}/D_{OBp}$	−/−/+/−
4	$D_{OCp}/D_{OBu}/D_{OBp}/A_{OBa}$	−/+/−/−
4	$D_{OCp}/A_{OCa}/D_{OBp}/A_{OBa}$	+/+/+/−
4	$D_{OCp}/A_{OCa}/D_{OBp}/A_{OBa}$	−/−/+/−
5	$D_{OCp}/A_{OCa}/D_{OBu}/D_{OBp}/A_{OBa}$	−/−/+/−/−
5	$D_{OCp}/A_{OCa}/D_{OBu}/D_{OBp}/A_{OBa}$ *	+/+/+/−/−

proposed for this particular ligand expression profile. Our numerical results suggest that this particular ligand expression profile (denoted here as Model structure 2), allows BMUs to be most functionally responsive (i.e. it produces the greatest change in bone volume in response to changes in differentiation rates).

Once this optimal model structure is identified, we then searched the model parameter space for combinations of differentiation and apoptosis rates which lead to a physiologically sensible system control responses. It turns out that a large range of parameter combinations leads to physiological unrealistic behaviours, such as exponential changes in bone volume, or only weak changes over the entire parameter range examined. However, a small number of parameter combinations could be identified leading to a physiological response that was close to a postulated idealised physiological response. Most interestingly, two of these parameter combinations are related to up-regulation of differentiation rate of osteoblast progenitors, down-regulation of differentiation rate of osteoblast precursors, and up-regulation of apoptosis rate of active osteoclasts as a parameter subset. This latter parameter modulation in differentiation rates corresponds to the known biological action of TGF-β, thereby providing at least a partial explanation for its particular suite of physiological actions in bone.

Acknowledgments

The authors are grateful to the Australian Research Council (ARC) for Fellowship funding (DP0559377).

References

[1] Lemaire V, Tobin FL, Greller LD, Cho CR, Suva LJ. Modeling the interactions between osteoblast and osteoclast activities in bone remodeling. J Theor Biol 2004;229: 293–309.
[2] Mundy GR. Cellular and molecular regulation of bone turnover. Bone 1999;24:35S–8S.
[3] Parfitt AM. Targeted and nontargeted bone remodeling: relationship to basic multicellular unit origination and progression. Bone 2002;30:5–7.
[4] Martin RB. Is all cortical bone remodeling initiated by microdamage? Bone 2002;30:8–13.
[5] Burr DB. Targeted and nontargeted remodeling. Bone 2002;30:2–4.
[6] Martin GR, Burr DB, Sharkey NA. Skeletal tissue mechanics. New York, USA: Springer; 1998.
[7] Rodan GA, Martin TJ. Therapeutic approaches to bone diseases. Science 2000;289:1508–14.
[8] Aubin JE. Advances in the osteoblast lineage. Biochem Cell Biol 1998;76:899–910.
[9] Aubin JE. Bone stem cells. J Cell Biochem Sublements 1998;30:73–82.
[10] Teitelbaum SL. Bone resorption by osteoclasts. Science 2000;289:1504.
[11] Martin TJ. Paracrine regulation of osteoclast formation and activity: milestones in discovery. J Musculoskelet Neuronal Interact 2004;4:243–53.
[12] Hofbauer LC, Kuehne CA, Viereck V. The OPG/RANKL/RANK system in metabolic bone diseases. J Musculoskelet Neuronal Interact 2004;4:268–75.
[13] Robling RB, Castillo AB, Turner CH. Biomechanical and molecular regulation of bone remodeling. Annu Rev Biomed Eng 2006;8:6.1–6.44.
[14] Defranoux NA, Stokes CL, Young DL, Kahn AJ. In silico modeling and simulation of bone biology: a proposal. J Bone Miner Res 2005;20:1079–84.
[15] Ventura BD, Lemerle C, Michalodimitrakis K, Serrano L. From in vivo to in silico biology and back. Nature 2006;443:527–33.
[16] Kroll MH. Parathyroid hormone temporal effects on bone formation and resorption. Bull Math Biol 2000;62:163–88.
[17] Rattanakul C, Lenbury Y, Krishnamara N, Wollkind DJ. Modeling of bone formation and resorption mediated by parathyroid hormone: response to estrogen/PTH therapy. Biosystems 2003;70:55–72.
[18] Komarova SV. Mathematical model of paracrine interactions between osteoclasts and osteoblasts predicts anabolic action of parathyroid hormone on bone. Endocrinology 2005;146:3589–95.
[19] Komarova SV, Smith RJ, Dixon SJ, Sims SM, Wahl LM. Mathematical model predicts a critical role for osteoclast autocrine regulation in the control of bone remodeling. Bone 2003;33:206–15.
[20] Savageau MA. Biochemical systems analysis — a study of function and design in molecular biology. Massachusetts, USA: Addison-Wesley Pub. Co.; 1976.
[21] Janssens K, ten Dijke P, Janssens S, Van Hul W. Transforming growth factor-beta1 to the bone. Endocr Rev 2005;26:743–74.
[22] Mundy GR. Bone remodeling and its disorders. 2nd ed. London, England: Martin Dunitz Ltd; 1999.
[23] Roodman GD. Cell biology of the osteoclast. Exp Hematol 1999;27:1229–41.
[24] Boyle WJ, Simonet WS, Lacey DL. Osteoclast differentiation and activation. Nature 2003;423:337.
[25] Simonet WS, Lacey DL, Dunstan CR, Kelley M, Chang MS, Luthy R, et al. Osteoprotegerin: a novel secreted protein involved in the regulation of bone density. Cell 1997;89:309–19.
[26] Bell NH. RANKL and the regulation of skeletal remodeling. J Clin Invest 2003;111: 1120–2.
[27] Hofbauer LC, Khosla S, Dunstan CR, Lacey DL, Boyle WJ, Riggs BL. The roles of osteoprotegerin and osteoprotegerin ligand in the paracrine regulation of bone resorption. J Bone Miner Res 2000;15:2–12.
[28] Hofbauer LC, Neubauer A, Heufelder AE. Receptor activator of nuclear factor-$\ka \be$ ligand and osteoprotegrin. Cancer 2001;92:460–70.
[29] Hofbauer LC, Schoppet M. Clinical implications of the osteoprotegerin/RANKL/RANK system for bone and vascular diseases. JAMA 2004;292:490–5.
[30] Cohen MM. Transforming growth factor beta's and fibroblast growth factors and their receptors: role in sutural biology and craniosynostosis. J Bone Miner Res 1997;12:322–31.
[31] Bonewald LF, Dallas SL. Role of active and latent transforming growth factor beta in bone formation. J Cell Biochem Sublements 1994;55:350–7.
[32] Seyedin SM, Thomas TC, Thompson AY, Rosen DM, Piez KA. Purification and characterization of two cartilage-inducing factors from bovine demineralized bone. PNAS 1985;82:2267–71.
[33] Hauschka P, Mavrakos A, Iafrati M, Doleman S, Klagsbrun M. Growth factors in bone matrix. Isolation of multiple types by affinity chromatography on heparin-sepharose. J Biol Chem 1986;261:12665–74.
[34] Erlebacher A, Filvaroff EH, Ye JQ, Derynck R. Osteoblastic responses to TGF-beta during bone remodeling. Mol Biol Cell 1998;9:1903–18.
[35] Fuller K, Lean J, Bayley K, Wani M, Chambers T. A role for TGFbeta(1) in osteoclast differentiation and survival. J Cell Sci 2000;113:2445–53.
[36] Gori F, Hofbauer LC, Dunstan CR, Spelsberg TC, Khosla S, Riggs BL. The expression of osteoprotegerin and RANK ligand and the support of osteoclast formation by stromal-osteoblast lineage cells is developmentally regulated. Endocrinology 2000;141:4768–76.
[37] Hofbauer LC, Dunstan CR, Spelsberg TC, Riggs BL, Khosla S. Osteoprotegerin production by human osteoblast lineage cells is stimulated by vitamin D, bone morphogenetic protein-2, and cytokines. Biochem Biophys Res Commun 1998;250:776–81.
[38] Udagawa N, Takahashi N, Jimi E, Matsuzaki K, Tsurukai T, Itoh K, et al. Osteoblasts/stromal cells stimulate osteoclast activation through expression of osteoclast differentiation factor/RANKL but not macrophage colony-stimulating factor. Bone 1999;25:517–23.
[39] Lauffenburger DA, Linderman JJ. Receptors: models for binding, trafficking, and signaling. New York, USA: Oxford University Press; 1993.
[40] Alon U. An introduction to systems biology: design principles of biological circuits. New York, USA: Chapman and Hall; 2007.
[41] Riggs BL, Parfitt AM. Drugs used to treat osteoporosis: the critical need for a uniform nomenclature based on their action on bone remodeling. J Bone Miner Res 2005;20:177–84.
[42] Glass II DA, Bialek P, Ahn JD, Starbuck M, Patel MS, Clevers H, et al. Canonical Wnt signaling in differentiated osteoblasts controls osteoclast differentiation. Dev Cell 2005;8:751–64.
[43] Thomas G, Baker S, Eisman J, Gardiner E. Changing RANKL/OPG mRNA expression in differentiating murine primary osteoblasts. J Endocrinol 2001;170:451–60.
[44] Huang JC, Sakata T, Pfleger LL, Bencsik M, Halloran BP, Bikle DD, et al. PTH differentially regulates expression of RANKL and OPG. J Bone Miner Res 2004;19: 235–44.